Open access • Journal Article • DOI:10.1109/TAP.1984.1143181

End-fire hybrid array antennas

W. Kahn

Institutions: George Washington University

Published on: 01 Jan 1984 - IEEE Transactions on Antennas and Propagation (IEEE)

Topics: Array gain, Reflective array antenna, Sensor array, Directional antenna and Antenna (radio)

End-Fire Hybrid Array Antennas

WALTER K. KAHN, FELLOW, IEEE

Abstract—**A heuristic approach useful in the design of end-fire array antennas is described. When an array is scanned "beyond end fire," the last elements of the array, in the direction of the end-fire beam, generally receive net power transmitted by other elements of the array. This received power might conceivably be recirculated and reradiated at the price of substantial complexity in the feed network. It is relatively simple to absorb this power in appropriate resistive loads at the price of reduced gain. The resulting end-fire antenna is a hybrid-array consisting of two classes of elements: elements excited directly and elements excited parasitically. A compromise termination of these parasitic elements in reactive loads especially determined to preserve desired pattern characteristics is examined.**

INTRODUCTION

THIS PAPER describes a heuristic approach useful in design of end-fire hybrid-array antennas [1], [2]. Hybrid arrays comprise two classes of elements: elements excited by generators either directly or through a feed network, and elements that are only excited parasitically as in the case of Yagi directors, Fig. 1. Excitation of elements in the first class can, at least in principle, be set arbitrarily. Excitation of elements in the second class is severely constrained. A simple procedure is presented for modifying an initial current distribution prescribed with certain pattern objectives in mind, to fit both hybrid array constraints and the lossless constraint. The pattern produced by the modified current distribution is then compared with that produced by the initially prescribed currents.

Current distributions for end-fire linear arrays are commonly derived as follows. A broadside pattern with the desired general characteristics is synthesized in direction cosine space. The main beam of the pattern is then scanned to end fire by means of a linear phase taper. With closely spaced arrays, a narrowing of the end-fire beam (increased directivity) may be obtained at the expense of higher relative sidelobe level by continuing to scan the main beam "beyond end fire" into the invisible region of direction cosine space [3]. We will see that such current distributions fit the hybrid array configuration rather naturally.

When prescribed currents are impressed on the fixed mutual impedance constraint of a linear array, definite voltages appear at the antenna terminals. If these currents are phased to scan the main beam beyond end fire, voltages at several of the antennas will be found to be more than 90° out of phase with the prescribed currents. This means that these antennas *receive* power from the others and, viewed at their terminals, appear as active circuit elements. In the case of these active elements, we have the following choices. We may seek to elaborate a network that accepts the received power and feeds it back into the elements that radiate net power, or we may absorb the received power in the appropriate passive load. The second alternative, which leads to one kind of hybrid antenna, is certainly much simpler (Fig. 1). However, power lost in the loads reduces the absolute gain of the array antenna even if the directivity of the radiation patterns remains constant. We propose to modify the prescribed currents so as to eliminate this loss. The passive loads corresponding to the modified currents will then be purely reactive. Among the infinite number of possible modifications that might accomplish this, we choose one that changes the prescribed current phasor by a small (the smallest) phasor increment. The intent, of course, is also to produce only a small change in the desirable pattern characteristics. If in particular the directivity (beamwidth) of the pattern is substantially maintained, the elimination of loss increases the absolute gain, restoring the design value.

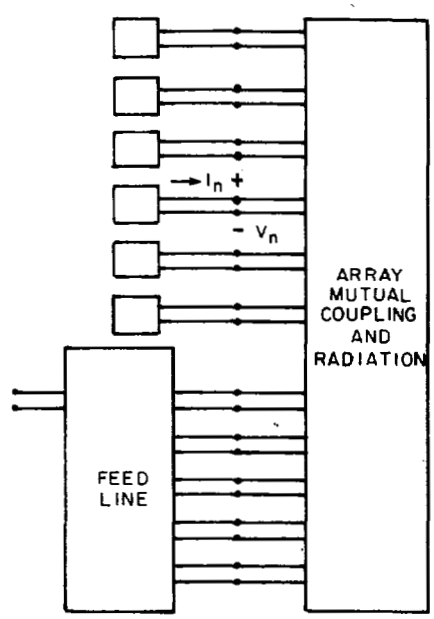

Fig. 1. Equivalent circuit of a hybrid antenna.

A network formulation of the array problem is outlined in the next section. Two ways of calculating the modified currents are given: a recursive algorithm, and a direct algebraic (matrix) solution. The recursive algorithm is advantageous for numerical computation.

A later section comprises two numerical examples. The uniform current distribution is examined as a classic despite the fact that the associated sidelobe level may be too high for most applications. A cosine-on-pedestal distribution illustrates the low sidelobe case.

NETWORK FORMULATION

A given arrangement of antennas in space results in a definite open-circuit impedance matrix characterizing the mutual inter-

Manuscript received March 9, 1983; revised July 20, 1983. This work is based on a report by the author, "End-fire hybrid array antennas," Airborne Radar Branch, Radar Division, Naval Research Laboratory, Washington, DC.

The author is with the Naval Research Laboratory, Washington, DC 20375 and the George Washington University, Washington, DC 20052.

actions of the array elements at the terminals of the antennas:

$$V_m = \sum_{n=1}^{N} Z_{mn} I_n. \tag{1}$$

These equations apply at the terminals of the array network shown on the right in Fig. 1. The positive directions for terminal voltage and current are indicated on that figure.

The complete radiation pattern of an array can be computed if the pattern radiated by an elementary antenna in the presence of all the other elements is known. When the other elements (which are not excited) are open circuited, the element field patterns in "open-circuited array environment," $f_{I,n}^{(0)}(\theta, \phi)$, are produced by unit currents. The total radiation field pattern produced when current I_n flows into the terminal of the nth antenna element, $n = 1, 2, \cdots, N$, is then found by superposition.

$$F(\theta, \phi) = \sum_{n=1}^{N} f_{I,n}^{(0)}(\theta, \phi) I_n. \tag{2}$$

Since, by definition, Z_{nn} is the input impedance to the nth antenna in the open-circuited array environment, the specification of unit current excitation implies the power normalization for $f_{I,n}^{(0)}(\theta, \phi)$

$$\iint_{\text{all angles}} |f_{I,n}^{(0)}(\theta, \phi)|^2 \, d\Omega = \text{Re}\{Z_{nn}\}. \tag{3}$$

Suppose a desired pattern $F(\theta, \phi)$ is obtained with some prescribed set of current I_n. Then, via (1), definite terminal voltages V_n appear as a response. In other words, effective input impedances

$$Z_{(n)} = \frac{V_n}{I_n}\bigg|_{\substack{\text{all } I_m \text{ prescribed, where} \\ m=1,2,\cdots,n,\cdots,N.}} \tag{4}$$

arise at the input of each antenna. The phase of the voltage V_n relative to the current I_n determines the direction of net (average) power. A particular antenna appears

$$\text{passive if } \text{Re}\{Z_{(n)}\} > 0, \tag{5a}$$

and

$$\text{active if } \text{Re}\{Z_{(n)}\} < 0. \tag{5b}$$

Power from one or more coherent generators must be supplied by a feed network to all elements which appear passive. The reader should be alert to a terminological difficulty. The antenna elements, which in the above technical network sense act as passive loads since they absorb power from the feed, are conventionally regarded as being thereby "activated." There seems to be no escape from this difficulty except to make clear what is meant here. The precise feed network need not be specified now.

When can negative values of $\text{Re}\{Z_{(n)}\}$ be expected? They arise in current distributions scanned "beyond end fire." Because of mutual coupling, the end elements in the direction of scan absorb rather than radiate net power and therefore in the technical network sense appear as active elements at their terminals. We choose to terminate each of these in an appropriate passive load. There are the individual loads at the upper left side of Fig. 1.

Appropriate Termination of Active Elements

As noted above, the definite mutual impedances between the given array element produces the voltage V_n at the nth port in response to *all* the prescribed currents. These values of voltage and current are consistent with only one value of impedance for the termination at an active port, Fig. 2, namely,

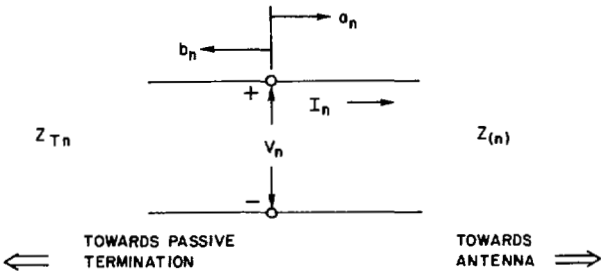

Fig. 2. Typical array antenna port, active input impedance.

$$Z_{Tn} = \frac{V_n}{-I_n} = -Z_{(n)}. \tag{6}$$

For n an active port, (5b) ensures that Z_{Tn} is passive.

Since $Z_{(n)}$ depends on the prescribed current distribution, so must the termination. Further, since the mutual coupling yielding $Z_{(n)}$ depends on frequency in some definite way, even the frequency dependence of Z_{Tn} must, in principle, follow. A different termination Z_{Tn}^a may be selected in place of Z_{Tn} only at the price of some deviation in the I_n, and consequently in the radiation pattern, from the prescribed values.

Reactive Terminations, Z_{Tn}^a

Compared to the terminations Z_{Tn} required at the active antenna ports for the prescribed currents, reactive terminations Z_{Tn}^a offer two advantages: one set of losses is eliminated from the array antenna, and the reactive terminations are easily realized in low loss transmission line leads. An algorithm leading to particular reactances and the corresponding perturbed currents is presented next.

The voltages V_n and currents I_n at the antenna terminals can be expressed in terms of wave amplitudes a_n incident onto the antenna and b_n reflected from the antenna

$$2\sqrt{R_{an}}\, a_n = V_n + R_{an} I_n \tag{7a}$$

$$2\sqrt{R_{an}}\, b_n = V_n - R_{an} I_n \tag{7b}$$

where R_{an} are normalization numbers. It will be convenient to take R_{an} equal to the characteristic impedance of the transmission line attached to the nth element. Each antenna element is assumed to have been tuned or matched to this characteristic impedance with all other antenna elements open-circuited.

Physically then, the waves b_n are produced by mutual coupling from the other antenna elements, especially those elements strongly excited by the feed network. To first order, this wave is treated as a constant. The wave a_n is regarded as due to reflection from the termination. The algorithm modifies this reflected wave to produce zero net power flow into the termination. We take the incident and reflected waves that obtain with the prescribed currents as zero order initial values in our algorithm and denote them $I_n^{(0)}$, $a_n^{(0)}$, $b_n^{(0)}$, etc. The composition of wave phasors a and b into the current phasor I,

$$\sqrt{R_g}\, I = a - b \tag{7c}$$

is shown in Fig. 3(a) (solid vectors.) Superscripts and subscripts have been dropped since the same construction can be applied at any stage of the algorithm and at any port. The proposed

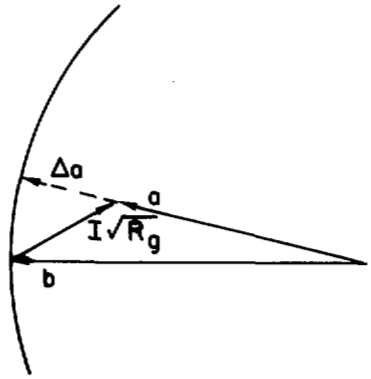

Fig. 3. Graphical illustration of algorithm synthesizing a reactive termination which minimizes the current increment, preserving the angle of the reflection coefficient.

modified value of a is shown dashed. The modified value of a is obtained by adding the smallest (magnitude) increment Δa that produces a resultant with the same magnitude as b. Clearly the smallest such increment Δa must be in phase with a; we may say the modification keeps the angle of the reflection coefficient b/a constant. For fixed b, Δa is direction proportional to a change in I, ΔI. The smallest $|\Delta a|$ therefore corresponds to the smallest $|\Delta I|$. The argument is approximate since, actually, b_n does depend on all the $a_m, m = 1, \cdots, N$.

From any given set of incident and reflected waves we compute a modified set as follows:

$$\left.\begin{aligned} a_n^{(s)'} &= a^{(s)} \\ b_n^{(s)'} &= b^{(s)} \end{aligned}\right\} \text{ passive ports,} \tag{8a}$$

$$\left.\begin{aligned} a^{(s)'} &= |\Gamma_{(n)}^{(s)}|\, a^{(s)} \\ b^{(s)'} &= b^{(s)} \end{aligned}\right\} \text{ active ports,} \tag{8b}$$

where the effective reflection coefficient

$$\Gamma_{(n)}^{(s)} = \frac{b_n^{(s)}}{a_n^{(s)}}. \tag{9}$$

The modified set of waves leads to new currents (at the active ports)

$$\sqrt{R_{gn}}\, I_n^{(s+1)} = a_n^{(s)'} - B_n^{(s)'}. \tag{10}$$

These new currents lead to an entirely new set of voltages $V_n^{(S+1)}$ via (2). The new voltages and currents define new incident and reflected waves $a^{(S+1)}$ and $b^{(s+1)}$ via (7). Starting with the prescribed currents $s = 0$ the process may be repeated until $|\Gamma_{(n)}^{(s)}|$ is sufficiently close to unity for all active ports. Occasionally the new current distribution may have the effect of turning a previously passive antenna element into an active one. In the examples studied, this algorithm was found to converge rapidly.

The constraint of maintaining the angle of the reflection coefficient may also be used in a direct calculation of the modified currents. We rewrite (2) in matrix form:

$$\mathbf{V} = \begin{pmatrix} \mathbf{V}_\alpha \\ \hdashline \mathbf{V}_\beta \end{pmatrix} = \left(\begin{array}{c:c} Z_{\alpha\alpha} & Z_{\alpha\beta} \\ \hdashline Z_{\beta\alpha} & Z_{\beta\beta} \end{array}\right) \begin{pmatrix} \mathbf{I}_\alpha \\ \hdashline \mathbf{I}_\beta \end{pmatrix} = Z\mathbf{I}, \tag{11}$$

where the matrices are partitioned to separate out quantities relating passive elements α and quantities relating to active elements β. Inserting the prescribed currents $\mathbf{I}^{(0)}$, we find the voltages $\mathbf{V}^{(0)}$ and the reflection coefficients $\Gamma_n^{(0)}$ as before. The *angles* of these reflection coefficients are used to compute reactive loads.

$$Z_{(n)}^{(h)} = \frac{|\Gamma_{(n)}^{(0)}| + \Gamma_{(n)}^{(0)}}{|\Gamma_{(n)}^{(0)}| - \Gamma_{(n)}^{(0)}}, \tag{12}$$

for all active elements in the hybrid antenna. These reactances are ordered into a diagonal square matrix,

$$Z_{\beta\beta}^{(h)} = \text{diag}\,\{Z_{(n)}^{(h)}\}. \tag{13}$$

Now

$$Z_{\beta\beta}^{(h)} \mathbf{I}_\beta^{(h)} = Z_{\beta\alpha}\mathbf{I}_\alpha^{(0)} + Z_{\beta\beta}\mathbf{I}_\beta^{(h)}, \tag{14}$$

where $\mathbf{I}_\beta^{(h)}$ are the desired modified currents at the active element ports. Solving for

$$\mathbf{I}_\beta^{(h)} = (Z_{\beta\beta}^{(h)} - Z_{\beta\beta})^{-1} Z_{\beta\alpha}\mathbf{I}_\alpha^{(0)}. \tag{15}$$

Although this formulation is attractive algebraically, problems of computational accuracy arise.

Transmission Loss, Efficiency

The efficiency factor to be evaluated here accounts for the power dissipated in the terminations Z_{Tn}. In the first instance, it represents the price paid for reducing size and complexity of the feed network so that it connects only to the passive array elements. It translates directly into decreased absolute antenna gain.

To obtain an upper bound efficiency, we assume that the feed network has no internal dissipation and that reflection losses at the input to the feed network have been eliminated by proper design. Therefore, the input power is the power absorbed by the passive array elements:

$$P_{IN} = \sum_{\substack{\text{passive} \\ \text{ports}}} |I_n|^2 \,\text{Re}\, Z_{(n)} = \sum_{\substack{\text{passive} \\ \text{ports}}} \{|a_n|^2 - |b_n|^2\}. \tag{16}$$

The power lost in the terminations attached to the active elements is

$$P_{TL} = \sum_{\substack{\text{active} \\ \text{ports}}} |I_n|^2 \,\text{Re}\, Z_{Tn} = \sum_{\substack{\text{active} \\ \text{ports}}} \{|b_n|^2 - |a_n|^2\}. \tag{17}$$

The efficiency factor, accounting for this loss in power actually radiated P_{rad}, is

$$\eta = \frac{P_{\text{rad}}}{P_{\text{in}}} = 1 - \frac{P_{TL}}{P_{IN}}. \tag{18}$$

It is convenient to express this efficiency as an equivalent transmission coefficient in decibels,

$$\text{dB}\, T = 10 \log_{10} \eta. \tag{19}$$

NUMERICAL RESULTS: A PLANAR ARRAY OF LINE SOURCES

To demonstrate the utility of the algorithm developed in the preceding section for realization of a lossless hybrid antenna design, the theory is now applied to an array of equally spaced line sources. This configuration was selected because of its simplicity and because it models an array of interest in connection with a specific airborne radar application. Two sets of prescribed initial current distributions are considered: a uniform distribution and a cosine-on-pedestal distribution.

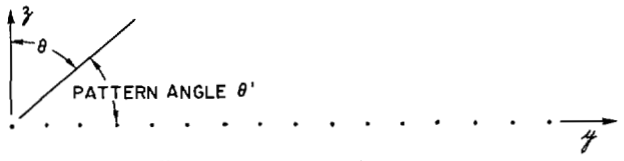

Fig. 4. Linear array of line sources.

Consider the array of N line sources shown in Fig. 4. The line currents extend indefinitely in the x direction. The elements are uniformly spaced along the y axis, D wavelengths apart. Adapted to this two-dimensional case, (1) for the radiation field becomes

$$F(\theta) = \sum_{n=1}^{N} f_{I,n}^{(0)}(\theta) I_n. \tag{20}$$

For idealized line sources the element patterns in the open-circuited array environment are all identical and isotropic. Consequently,

$$\sqrt{2\pi} F(\theta) = \sum_{n=1}^{N} I_n e^{j2\pi(n-1)D \sin\theta}, \tag{21}$$

where the exponential factor accounts for the relative location of the elements. The elements of the open circuit impedance matrix are known [5], [6]

$$Z_{mn} = 1, m = n, \tag{22a}$$

$$Z_{mn} = H_0^{(2)}(2\pi D\,|m-n|), \quad m \neq n; \tag{22b}$$

where $H_0^{(2)}$ is the zeroth-order Hankel function of the second kind.

A classic distribution consists of currents with uniform amplitude and linearly progressive phase:

$$I_n = e^{-j\beta(n-1)}. \tag{23}$$

The peak of the resulting radiation pattern, corresponding to in-phase addition of radiation from each element, occurs at values of θ such that

$$2\pi D \sin\theta - \beta = 2\pi\nu \tag{24}$$

where ν is any integer. This is located at end fire, say $\theta = \pi/2$, when $\beta = 2\pi D$. All the values of $\sin\theta$ for in-phase addition are in Fig. 5(a). This particular figure has been drawn using $D = 0.333$. For values of D less than one-half wavelength, $D < 0.5$, there is a range of β for which the in-phase addition peak is placed in the invisible region,

$$1 < \left|\frac{\beta}{2\pi D}\right| < \frac{1}{D} - 1. \tag{25}$$

When β is in this range, the actual beam is narrowed to the portion left in visible space, $-1 < \sin\theta < +1$, and the relative sidelobe level appears correspondingly raised (Fig. 5(b)).

An alternative way of stating the same condition (in terms of the total phase shift across the antenna aperture) is conventional for surface wave antennas,

$$\Phi = [\beta - 2\pi D](N-1), \tag{26}$$

where Φ is the excess phase shift of the surface wave over the aperture compared to the phase shift that would be experienced by a plane wave traversing the same aperture. The Hansen-Woodyard condition for enhanced end-fire gain corresponds to an excess phase Φ of 180° [3].

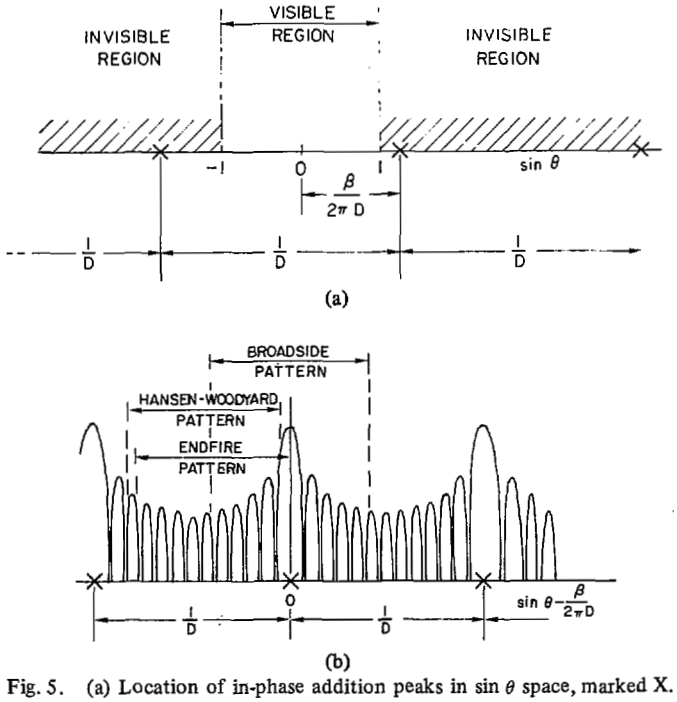

Fig. 5. (a) Location of in-phase addition peaks in $\sin\theta$ space, marked X. (b) Relationship of broadside end fire and Hansen-Woodyard patterns.

For an array of 16-line currents ($N = 16$), spaced one-third wavelength apart ($D = 0.333$), direct computation shows that all antenna elements remain passive for values of Φ less than about 150°. For $\Phi = 200°$, the first ten elements are passive and the remaining six appear active. Specifically, the input reflection coefficients $\Gamma_{(n)}$ at the inputs to the 16 antenna elements are listed in the upper part of Table I together with the prescribed uniform current distribution which gave rise to them. The perturbed distribution obtained by applying our algorithm is listed in the lower part of the table. It will be seen that elements 11 through 16 now have reflection coefficients of magnitude unity. These elements are passive and can be terminated in reactances Z_{Tn}. The corresponding power patterns are shown in Fig. 6. The solid curve corresponds to the prescribed currents while the broken curve is obtained using the new currents. The half-power beamwidth is not substantially changed while the sidelobe level has increased from the original value of −7.4 to −6.8 dB. Assuming the active elements terminated in passive loads, the original distribution is associated with an efficiency (loss factor) of −0.83 dB. This loss is eliminated by the hybrid distribution. Assuming no change in antenna directivity (possibly a somewhat optimistic estimate in view of the high sidelobe level present in this case) the antenna gain would be enhanced by the same +0.83 dB.

The second distribution to be considered consists of currents with symmetrically tapered amplitudes and linearly progressive phase:

$$I_n = \left[0.55 - 0.45\cos\frac{2\pi}{(N-1)}(n-1)\right] e^{-j\beta(n-1)}, \tag{27}$$

a cosine-on-pedestal distribution. The peak of the resulting pattern corresponding to in-phase addition of radiation from each element is positioned by the choice of β. As discussed previously,

TABLE I
END-FIRE ARRAY OF LINE SOURCES

Prescribed Current Distribution: Uniform				
Currents, I_n			Reflection Coefficients, $\Gamma_{(n)}$	
Absolute, dB	Degrees	n	Absolute	Degrees
0.000	0.000	1	.317	−179.247
0.000	−133.213	2	.278	84.168
0.000	93.573	3	.353	65.976
0.000	−39.639	4	.500	64.522
0.000	−172.853	5	.619	54.391
0.000	53.933	6	.642	51.261
0.000	−79.279	7	.726	54.473
0.000	147.506	8	.836	50.219
0.000	14.293	9	.840	48.240
0.000	−118.919	10	.898	52.883
0.000	107.866	11	1.036	50.657
0.000	−25.346	12	1.024	48.197
0.000	−158.559	13	1.046	55.082
0.000	68.226	14	1.281	55.343
0.000	−64.986	15	1.232	49.365
0.000	161.800	16	1.071	61.062
Modified Current Distribution				
−.962	0.000	1	.342	177.522
−.962	−133.213	2	.282	80.458
−.962	93.573	3	.337	65.871
−.962	−39.639	4	.509	66.104
−.962	−172.853	5	.627	53.301
−.962	53.933	6	.628	50.919
−.962	−79.279	7	.732	55.764
−.962	147.506	8	.847	49.339
−.962	14.293	9	.823	47.741
−.962	−118.919	10	.902	54.652
−.752	111.118	11	1.000	50.180
−.903	−24.432	12	1.001	47.087
−.748	−155.900	13	.997	57.568
0.000	83.765	14	1.004	58.062
−.084	−48.499	15	1.005	47.068
−.270	170.592	16	1.008	55.390

Element Spacing, $D = 0.333$
Excess Phase Across Aperture, $\Phi = 200°$

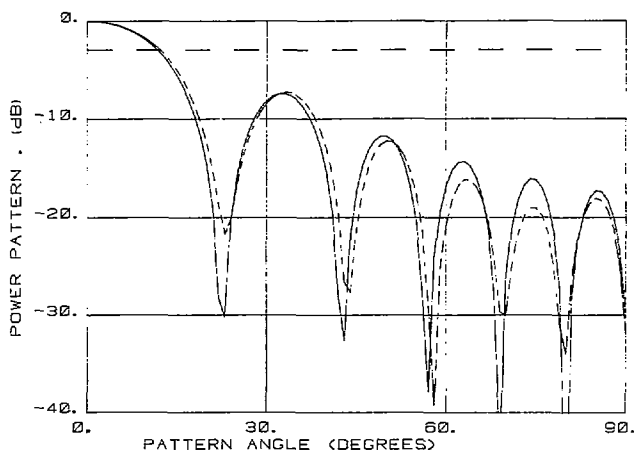

Fig. 6. Power pattern—uniform distribution; excess phase delay aperture = 200°, $D = 0.333$.

the end-fire beam may be narrowed through an excess progressive shift across the aperture.

For an array of 16-line currents ($N = 16$) spaced one-third wavelength apart ($D = 0.333$), direct computation shows that for $\Phi = 350°$, the first 10 elements remain passive while the remaining six elements appear active. Specifically, the input reflection coefficients $\Gamma_{(n)}$ at the inputs to the 16 antenna elements are listed in the upper part of Table II together with the prescribed cosine-on-pedestal current distribution. In the lower part of the table we list the modified distribution obtained by applying an algorithm (8), (9), and (10). Elements 11 through 16 finally have reflection coefficients of magnitude unity. Power patterns are shown in Fig. 7(e). The solid curve corresponds to

TABLE II
END-FIRE ARRAY OF LINE SOURCES

Prescribed Current Distribution Cosine on Pedestal				
Currents, I_n			Reflection Coefficients, $\Gamma_{(n)}$	
Absolute, dB	Degrees	n	Absolute	Degrees
−20.000	0.000	1	.213	−175.929
−17.145	−143.213	2	.307	145.823
−12.079	73.573	3	.426	131.296
−7.724	−69.639	4	.439	115.831
−4.479	147.146	5	.455	105.448
−2.213	3.933	6	.514	97.175
−.780	−139.279	7	.596	88.363
−.085	77.506	8	.677	80.749
−.085	−65.706	9	.775	75.322
−.780	151.080	10	.918	69.670
−2.213	7.866	11	1.092	61.818
−4.479	−135.346	12	1.291	52.555
−7.724	81.440	13	1.552	38.857
−12.079	−61.773	14	1.623	17.727
−17.145	155.013	15	1.434	3.159
−20.000	11.799	16	1.338	−6.648
Modified Current Distribution				
−19.914	0.000	1	.242	−178.276
−17.059	−143.213	2	.305	141.281
−11.993	73.573	3	.411	131.764
−7.638	−69.639	4	.441	116.959
−4.394	147.146	5	.460	105.164
−2.128	3.933	6	.512	96.735
−.694	−139.279	7	.593	88.670
0.000	77.506	8	.681	80.865
0.000	−65.706	9	.774	74.973
−.694	151.080	10	.914	70.093
−1.741	12.323	11	1.000	64.186
−3.560	−119.982	12	1.013	54.658
−7.210	115.265	13	1.008	37.997
−15.302	−1.897	14	1.003	15.615
−31.998	−116.934	15	1.000	2.548
−27.325	−56.355	16	.989	−4.770

Element Spacing, $D = 0.333$
Excess Phase Across Aperture, $\Phi = 350°$

the prescribed currents, and the broken curve to the new perturbed currents.

The remaining parts of Fig. 7 display patterns obtained with the same configuration $N = 16$, $D = 0.333$, for various values of excess phase: $\Phi = 250°$, 275°, 300°, 325°, 375°, and 400°. The expected trends, narrowing of the main beam accompanied by a rising sidelobe level, are evident. Pattern characteristics are compared in Table III.

Finally, the value of the perturbed illumination would be curtailed if the reactive terminations required by the perturbed illumination was highly frequency sensitive. In fact, mutual coupling effects do not lead to a rapid change with frequency. The dependence of the phase of the required load reflection coefficient for the cosine-on-pedestal distribution as a function of the element spacing in fractional wavelengths is listed in Table IV. Both the nominal values and the final values arising from the algorithm used to compute the hybrid currents are given. The excess phase is kept constant, $\Phi = 350°$. The patterns corresponding to $D = 0.300$ and $D = 0.366$ are shown in Figs. 8(a) and 8(b).

CONCLUSION

When an array antenna is scanned "beyond end fire" to achieve a degree of superdirective narrowing of the pattern, the direction of power in some of the antenna elements may reverse. In particular, the last elements of the array in the direction of the end-fire beam tend to receive power transmitted by the

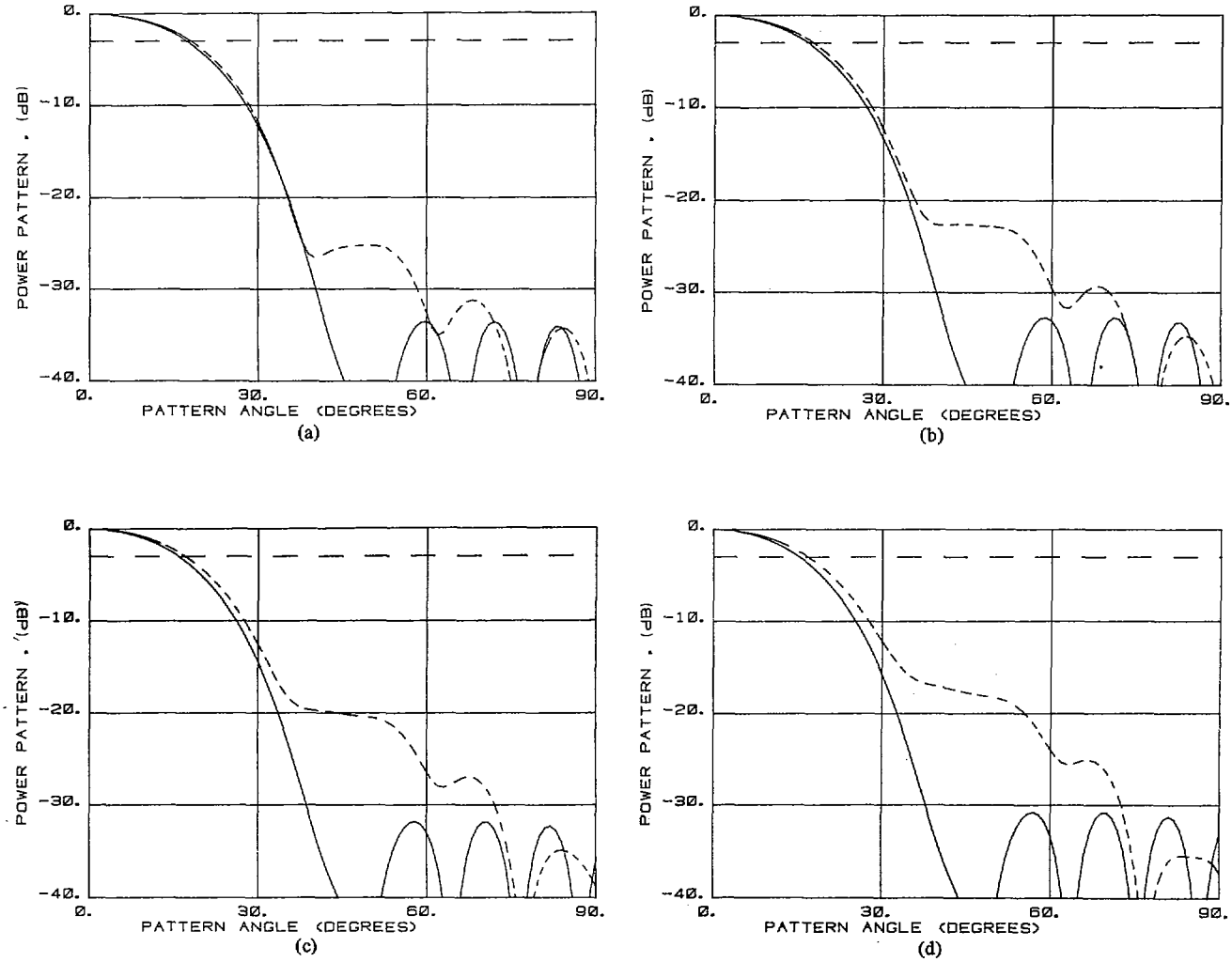

Fig. 7. (a) Power pattern–cosine on pedestal: prescribed current ——, reactive loads ---, excess phase across aperture = 250°, D = 0.333 wavelength. (b) Power pattern–cosine on pedestal: prescribed current ——, reactive loads ---, excess phase across aperture = 275°, D = 0.333 wavelength. (c) Power pattern–cosine on pedestal: prescribed current ——, reactive loads ---, excess phase across aperture = 300°, D = 0.333 wavelength. (d) Power pattern–cosine on pedestal: prescribed current ——, reactive loads ---, excess phase across aperture = 325°, D = 0.333 wavelength. (e) Power pattern–cosine on pedestal: prescribed current ——, reactive loads ---, excess phase across aperture = 350°, D = 0.333 wavelength. (f) Power pattern–cosine on pedestal: prescribed current ——, reactive loads ---, excess phase across aperture = 375°, D = 0.333 wavelength. (g) Power pattern–cosine on pedestal: prescribed current ——, reactive loads ---, excess phase across aperture = 400°, D = 0.333 wavelength.

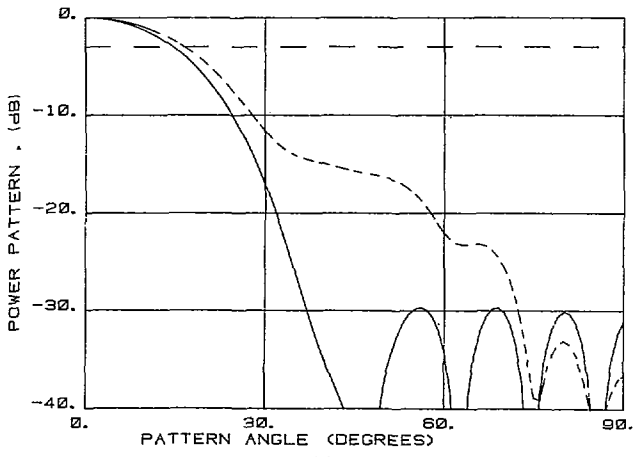

(e)

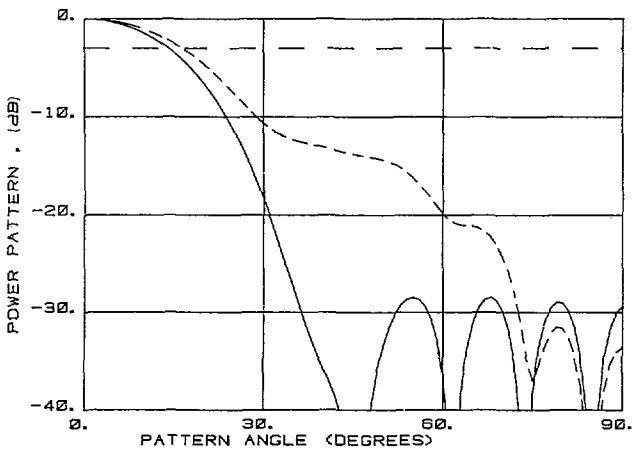

(f)

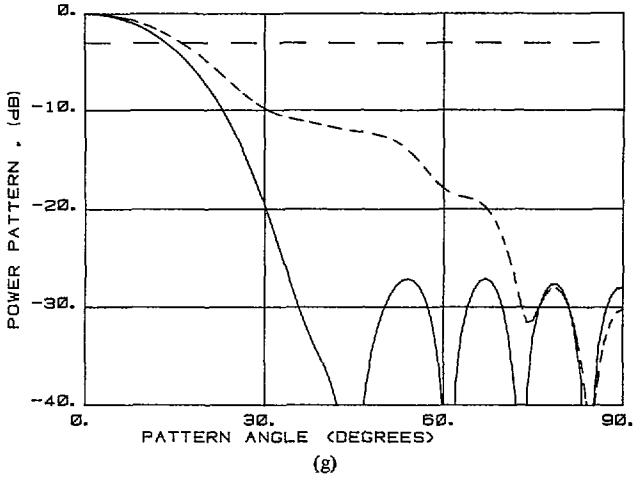

(g)

Fig. 7. (*Continued*)

TABLE III
COMPARATIVE PATTERN CHARACTERISTICS

Prescribed Cosine-on-Pedestal				Modified Illumination		
Excess Phase (deg)	Directivity (dB)	Loss (dB)	Gain (dB)	Gain (dB)	Δ Gain (dB)	Side-lobe* (dB)
250	10.2	−0.8	9.4	10.0	0.6	−25.2
275	10.4	−0.9	9.5	10.1	0.6	−22.6
300	10.5	−1.2	9.3	10.2	0.9	−20.0
325	10.8	−1.4	9.4	10.3	0.9	−17.8
350	11.0	−1.7	9.3	10.5	1.2	−15.5
375	11.1	−1.9	9.2	10.5	1.3	−13.0
400	11.2	−2.1	9.1	10.5	1.4	−11.4

*Cosine-on-pedestal side-lobe level < 25 dB

TABLE IV
ANGLE OF THE ACTIVE REFLECTION COEFFICIENT, ANGLE $\{\Gamma_{(n)}\}$

Element	Element Spacing					
	D = 0.300		D = 0.333		D = 0.366	
n	initial (deg)	final (deg)	initial (deg)	final (deg)	initial (deg)	final (deg)
11	63.5	66.3	61.8	64.2	60.2	62.6
12	51.6	53.1	52.6	54.7	53.0	55.0
13	36.8	36.0	38.9	38.0	39.8	39.1
14	16.3	14.1	17.7	15.6	20.0	17.9
15	2.3	1.8	3.2	2.5	4.0	3.2
16	−6.2	−5.9	−6.6	−4.8	−7.1	−6.3

other elements of the array. This received power might conceivably be recirculated, but is more conveniently absorbed in loads. The resulting loss must then be charged against the enhanced directivity in computing gain. The alternative studied in this report, a modification of the illumination which reduces the absorbed power to zero (reactive termination), preserves desired pattern characteristics to the extent shown in the power patterns of Figs. 7 and 8 and summarized in Table III.

Although the directivity is enhanced by about 1 dB when the beam is scanned beyond end fire, the enhanced directivity is accompanied by a slight loss in gain. The loss in gain may be offset by modifying the current distribution as discussed in the report. The optimum in terms of gain is then very broad. The rapid deterioration in the sidelobe level indicates that scan "beyond end fire" technique is subject to rapidly diminishing returns. More sophisticated modifications of the initial current distribution may soften this last conclusion.

ACKNOWLEDGMENT

The author is grateful to Dr. T. L. ap Rhys for his interest and valuable comments.

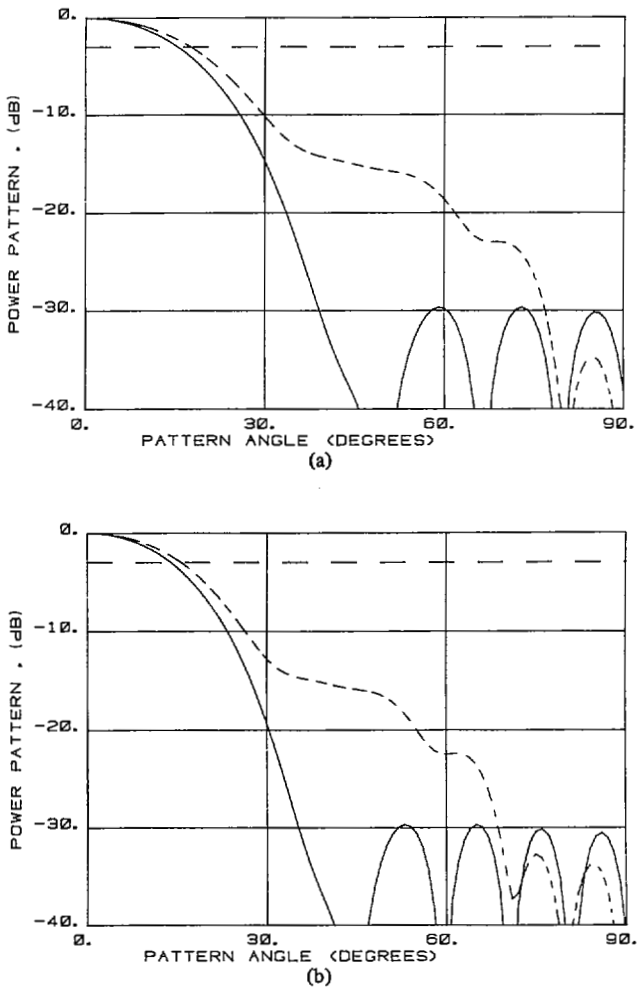

Fig. 8. (a) Power pattern–cosine on pedestal: prescribed current ——, reactive loads ---, excess phase across aperture = 350°, $D = 0.300$ wavelength. (b) Power pattern–cosine on pedestal: prescribed current ——, reactive loads ---, excess phase across aperture = 350°, $D = 0.366$ wavelength.

REFERENCES

[1] W. K. Kahn, "Center-fed leaky-wave Yagi hybrid antenna," *Navy Tech. Disclosure Bulletin*, vol. 3, no. 8, pp. 60–62, Aug. 1978.

[2] ——, "Double-ended backward-wave Yagi hybrid antenna," *IEEE Trans. Antennas Propagat.*, vol. AP-29, no. 3, pp. 530–532, May 1981.

[3] R. S. Elliott, *Microwave Scanning Antenna, II*, ch. I, R. C. Hansen, Ed. New York: Academic, 1966.

[4] W. Wasylkiwskyj, "Mutual coupling effects in semi-infinite arrays" *IEEE Trans. Antennas Propagat.*, vol. AP-21, no. 3, pp. 277–285, May 1973.

[5] W. Wasylkiwskyj and W. K. Kahn, "Coupling, radiation and scattering by antennas," in *Proc. Symp. Generalized Networks*, Apr. 12, 13, 14, 1966; Microwave Research Institute Symposia Series, 16; 83-14, Polytechnic Press of the Polytech. Inst. Brooklyn, 1966.

[6] ——, "Theory of mutual coupling among minimum scattering antennas," *IEEE Trans. Antennas Propagat.*, vol. AP-18, pp. 204–216, Mar. 1970.

Walter K. Kahn (S'50–A'51–M'56–SM'59–F'67) was born in Mannheim, Germany, on March 24, 1929. He received the B.E.E. degree from Cooper Union, New York, NY, in 1951, and the M.E.E. and D.E.E. degrees from the Polytechnic Institute of Brooklyn, Brooklyn, NY, in 1954 and 1960, respectively.

From 1951 to 1954 he was engaged in monopulse radar system development at Wheeler Laboratories, Hazeltine Corporation, Greenlawn, NY. Subsequently, he conducted research at the Polytechnic Institute on a wide range of topics within the microwave field, and was assistant to the director of the Microwave Research Institute and Professor of Electrophysics. He joined the Department of Electrical Engineering and Computer Science of the George Washington University, Washington, DC, in 1969 as a Professor of Engineering and Applied Science. He has served as a consultant to the Naval Research Laboratory, major industrial organizations and is a principal in ANRO Engineering Consultants, Bedford, MA. He is conducting research in array antennas and optics for laser applications.

Dr. Kahn was an elected member of the IEEE Antennas and Propagation Society Administrative Committee, and served as Editor of this TRANSACTIONS.